Cerebral Cortex December 2007;17:2949-2960
doi:10.1093/cercor/bhm021
Advance Access publication March 29, 2007

Laminar Specificity of Intrinsic Connections in Broca's Area

Eric Tardif[1,2], Alphonse Probst[3] and Stephanie Clarke[1]

[1]Service de Neuropsychologie et de Neuroréhabilitation, CHUV, Université de Lausanne, CH-1011 Lausanne, Switzerland, [2]Département de Biologie Cellulaire et de Morphologie, Université de Lausanne, CH-1011 Lausanne, Switzerland and [3]Institut für Pathologie, Universität CH-4002 Basel, Switzerland

Broca's area and its right hemisphere homologue comprise 2 cytoarchitectonic subdivisions, FDΓ and FCBm of von Economo C and Koskinas GN (1925, Die Cytoarchitektonik der Hirnrinde des erwachsenen Menschen. Vienna/Berlin [Germany]: Springer). We report here on intrinsic connections within these areas, as revealed with biotinylated dextran amine and 1,1′-dioctadecyl-3,3,3′,3′-tetramethylindocarbocyanine perchlorate tracing in postmortem human brains. Injections limited to supragranular layers revealed a complex intrinsic network of horizontal connections within layers II and III spreading over several millimeters and to a lesser extent within layers IV, V, and VI. Ninety percent of the retrogradely labeled neurons ($n = 734$) were in supragranular layers, 4% in layer IV, and 6% in infragranular layers; most were pyramids and tended to be grouped into clusters of approximately 500 μm in diameter. Injections involving layer IV revealed extended horizontal connections within layers I–IV (up to 3.7 mm) and to a lesser extent in layers V and VI. Injections limited to the infragranular layers revealed horizontal connections mainly limited to these layers. Thus, intrinsic connections within Broca's area display a strong laminar specificity. This pattern is very similar in areas FDΓ and FCBm and in the 2 hemispheres.

Keywords: BDA, cerebral cortex, DiI, human, inferior frontal gyrus, tracing

Introduction

Since the seminal observation of Broca (1861), numerous studies have confirmed that lesions in the left inferior frontal gyrus are associated with a wide range of speech deficits. Activation studies in normal subjects have also confirmed the key role of Broca's area in language functions (for reviews, see Price 2000; Bookheimer 2002; Hagoort 2005; Vigneau et al. 2006). Furthermore, several activation studies suggest that relatively small regions within and beyond the classically defined Broca's area may be associated with particular aspects of language processing (Bookheimer 2002; Vigneau et al. 2006). The homologue of Broca's area in the right hemisphere (i.e., the posterior part of the inferior frontal gyrus) may play a critical role in specific aspects of language processing, such as understanding metaphoric sentences (Bottini et al. 1994), judging semantic versus syntaxic anomalies (Kang et al. 1999), integration of semantic information (Caplan and Dapretto 2001), and prosody (Buchanan et al. 2000; Friederici 2001). The posterior parts of left and right inferior frontal gyri are also activated by a wide range of nonlanguage tasks including various aspect of motor processing (Iacoboni et al. 1999; Binkofski et al. 2000; Schubotz and von Cramon 2001; Grafton et al. 2002; Koski et al. 2002, 2003; Heiser et al. 2003; Binkofski and Buccino 2004), synchronization of movement with sensory events (Rao et al. 1997), perceptual analysis of temporal patterns (Schubotz et al. 2000), tone discrimination (Muller et al. 2001), cognitive analysis of musical structures (Maess et al. 2001), and the maintenance of objects in working memory (Mecklinger et al. 2002). Moreover, activation of Broca's area and its homologue in the right hemisphere during empathic states and imitation tasks suggests their involvement in a "mirror" system linking perceived and executed actions (Rizzolatti and Arbib 1998; Iacoboni et al. 1999; Chaminade et al. 2001; Carr et al. 2003; Leslie et al. 2004; Aziz-Zadeh et al. 2006).

Broca's area is located in the posterior part of the inferior frontal gyrus of the left hemisphere (Broca 1861; Galaburda 1980; Amunts et al. 1999; Horwitz et al. 2003) and more specifically in triangular and opercular parts that are defined macroscopically by the sulcal configuration. Cytoarchitectonically, Broca's area and its homologue in the right hemisphere comprise 2 areas, FCBm and FDΓ of von Economo and Koskinas (1925), corresponding to Brodmann's areas 44 and 45 (Brodmann 1909), respectively. Anatomical studies demonstrated hemispheric asymmetries within the posterior parts of the inferior frontal gyrus. Triangular and opercular parts tend to be larger on the left side (Foundas 1995; Foundas et al. 1996, 1998, 2001). Cytoarchitectonically, Brodmann's area 44 (Amunts et al. 1999; corresponding to area FCBm of von Economo and Koskinas 1925) and, in a different cytoarchitectonic subdivisions scheme, the inferofrontal magnopyramidal region (Braak 1979; Galaburda 1980) have been shown to be larger on the left side. The volume fraction of cell bodies in areas 44 and 45 (Amunts et al. 2003) and the size of layer III pyramidal neurons in area 45 (Hayes and Lewis 1995) were shown to be greater on the left side.

The involvement of Broca's area in a range of different functions raises the question of how the information is integrated within this area and whether Broca's area differs in this respect from its right counterpart. Work on the primary visual cortex in nonhuman primates showed that intrinsic cortical connectivity reflects the functional intraareal organization. Patchily distributed intrinsic connections in the primary visual area were shown to link predominantly compartments with the same functional specialization (Rockland and Lund 1983; Livingstone and Hubel 1984). Moreover, the patterns of intrinsic connectivity were shown to differ greatly following tracer injections in specific cortical layers and/or cortical areas (Lund et al. 1993). The intrinsic connectivity of Broca's area, and more generally of human prefrontal areas, has not been investigated before. Previous studies have explored visual areas V1 and V2 (Burkhalter and Bernardo 1989; Kenan-Vaknin et al. 1992) and the primary and association auditory areas (Galuske et al. 2000; Tardif and Clarke 2001; Hutsler and Galuske 2003). We report here on the intrinsic connectivity of Broca's area and

of its counterpart in the right hemisphere as revealed by postmortem tracing with biotinylated dextran amine (BDA) and 1,1′-dioctadecyl-3,3,3′,3′-tetramethylindocarbocyanine perchlorate (DiI). Particular attention was paid to neuronal types participating in intrinsic connectivity as well as patterns of connectivity originating from different cortical layers.

Materials and Methods

Intrinsic connections were studied in triangular and opercular parts of left and right inferior frontal gyri in 10 human brains, which were purveyed by the donor program at the Department of Cellular Biology and Morphology, Faculty of Biology and Medicine in Lausanne or through authorized autopsies at the Institute of Pathology, University of Basel. The recommendations of the Declaration of Helsinki were followed; the bequest of the body to the donor program involved written consent of the donor, and for brain autopsy, permission was obtained from patients' relatives. All subjects died from causes unrelated to the brain (Table 1). Absence of brain lesions was ascertained macroscopically on brain slices of the whole brain and within the frontal lobe microscopically on Nissl-stained sections. In addition, brains obtained at autopsy were examined for the presence of histopathological lesions using periodic acid methenamine silver for the detection of senile plaques; Gallyas silver iodide for the detection of neurofibrillary tangles, neuropil threads, and argyrophilic grains; and immunohistochemical method using antibodies against abnormally phosphorylated tau-protein and alpha-synuclein for the detection of neurofibrillary tangles and Lewy bodies and Lewy neurites. No pathological changes were found in Broca's area or in its right hemisphere homologue. Cases 1 and 3 had argyrophilic grains within the hippocampus and the entorhinal cortex. Case 2 had neurofibrillary tangles (corresponding to stage III and IV of Braak) in the entorhinal and transentorhinal cortices, hippocampus, and fusiform gyrus. Case 8 had Lewy bodies and neurites in the brainstem (vagal complex, locus coeruleus, and medial raphe nucleus), olfactory bulbs, amygdala, hippocampus, superior and middle temporal gyri, and cingulum.

Intrinsic connections have been traced with BDA (molecular weight 3000 or 10 000) or DiI.

Tracing with BDA

For BDA injections, the procedure adapted from Dai, Swaab, et al. (1998) and Dai et al. (1998a, 1998b) was used in the manner described in Tardif et al. (2005). The brain was removed from the skull and dampened with artificial cerebrospinal fluid (ACSF; NaCl, 120 mM; KCl, 3 mM; NaH_2PO_4, 1.4 mM; D-glucose, 10 mM, pH. 7.3) at 4 °C. Meninges covering inferior frontal gyri and surrounding regions were gently removed before photographs were taken with a numerical camera (Sony, DSC-S75), covering lateral, inferior, and inferolateral views of the inferior frontal gyrus and standard views of both hemispheres. Inferior frontal gyri were then dissected into triangular and opercular parts and immersed into ACSF supplied by 95% O_2 + 5% CO_2 for 2 h. A tissue block was then glued on a metallic plate and immersed in ACSF kept at 4 °C with surrounding ice cubes. A glass micropipette (tip from 1 to 5 μm diameter) containing 5% BDA held by a micromanipulator (WPI; Taurus, Berlin, Germany) was inserted perpendicularly in the cortex. Iontophoretic injections were made by using a 7-μA positive current with 7 s on and 7 s off over 5–10 min, yielding injections cores of approximately 300–800 μm in diameter, with very little diffusion around the injection site (Figs 1*C*,*E* and 2*A*). Injection locations were transposed on the photographs taken before dissection. Tissue blocks were then put in ACSF supplied by 95% O_2 + 5% CO_2 at room temperature for 12 h, and then fixed by immersion in 4% paraformaldehyde in 0.1 M phosphate buffer (pH. 7.4) for 7 days, followed by 20% sucrose in phosphate buffer until they sank. Blocks were then quickly frozen in isopentane, surrounded by dry ice, and kept at –20 °C until sectioning with a cryostat. Serial sections (40 μm) were collected in 0.05 M Tris buffer saline (TBS; 0.05 Tris, 0.9% NaCl, pH. 8.0). BDA tracing required keeping the tissue unfixed for more than 12 h, which rendered it delicate for subsequent histology. In particular, pial surface was prone to mechanical damage.

The BDA was revealed as follows: sections were rinsed in TBS, pH 8.0, 3 × 10 min and incubated 10 min in methanol 70% + 0.5% H_2O_2 to reduce intrinsic peroxidase activity. They were then rinsed in Tris buffer saline Tween (TBST; 50 mM Tris buffer (TB) + NaCl 0.9% + Tween 0.5%, pH. 8.0) 3 × 30 min before incubation in avidin–biotin–horseradish peroxidase complex (ABC kit; Vector, Peterborough, UK) in TBST for 130 min. Sections were rinsed in TB (50 mM, pH. 8.0) 4 × 20 min and put into TB with 0.4% nickel ammonium sulfate (pH 8.0). Sections were preincubated in TB with 0.4% nickel ammonium sulfate (pH 8.0) and 0.02% 3,3′-diaminobenzidine tetrahydrochloride (DAB) for 10 min. The same volume of TB with 0.4% nickel ammonium sulfate (pH 8.0), DAB 0.02%, and 0.003% H_2O_2 was then added for 20–30 min. Sections were rinsed in TB (pH. 8.0) 3 × 10 min, mounted on gelatine-coated glass slides, and then dehydrated and coverslipped. Regularly spaced sections were counterstained with cresyl violet.

Tracing with DiI

For DiI injections, tissue blocks were dissected and fixed immediately in 4% paraformaldehyde in phosphate buffer for 1 week. In 2 cases (9 and 10), brains were perfused through the internal carotid and the basilar arteries with heparin (5 mL in each artery) followed by a perfusion with 0.9% NaCl with heparin and then by 4% paraformaldehyde in phosphate buffer. A postfixation of 12 h was achieved by immersion in the same fixative. DiI was then applied either by placing a small crystal of DiI (diameter ca. 400 μm) below the pial surface with the tip of a micropipette or by 0.2 μL injections of 10% DiI dissolved in dimethylformamide. For the latter, a 1-μL Hamilton syringe, held by a micromanipulator (WPI; Taurus), was lowered perpendicularly to the pial surface into the cortical gray matter. Tissue blocks were then kept at room temperature or at 37 °C for 3–54 months. Blocks were embedded in 4% agar and serial 40-μm–thick sections were cut with a vibratome (Leica,

Table 1
Description of cases and location of injections

Case	Sex	Age (y)	TDF (h)	Cause of death; concurrent disease (if present)	Injections	
					Tracer	Cytoarchitectonic area (number of injections; cortical layers involved)
1	F	91	10	Pneumonia; cardiac failure	BDA 3 kDa	LFDΓ (2; I–III; I–III)
2	F	89	24	Cardiac failure	BDA 10 kDa	LFCBm (1; III–IV–**V**–VI), Ltrans (2; **V**–VI; I–III)
3	F	76	8	Cardiac failure; thyroid carcinoma	BDA 10 kDa	LFCBm (2; III–**IV**–V; III–**IV**–V), LFDΓ (1; III–**IV**–V), RFDΓ (3; III–**IV**–V; III–**IV**–V; IV–**V–VI**), RFCBm (1; I–**III**–IV)
4	M	70	16	Cardiac failure; bronchial carcinoma	DiI (crystalline)	LFDΓ (2; I–III; I–III); RFDΓ (1; I–III), RFCBm (1; I–III)
5	M	75	15	Myocardial infarction; renal carcinoma	DiI (crystalline)	LFDΓ (1; I–III), RFCBm (1; I–**III**–IV)
6	F	66	14	Bronchopneumonia; essential tremor	DiI (crystalline)	LFDΓ (1; I–III), LFCBm (1; I–III), RFCBm (1; I–III)
7	M	81	23	Bronchopneumonia; bronchial carcinoma	DiI (crystalline)	LFDΓ (1; I–III), RFDΓ (1; I–III)
8	M	84	10	Bronchopneumonia	DiI (crystalline)	LFDΓ (1; I–III), Ltrans (1; I–III), LFCBm (1; I–III)
9	M	82	10	Cardiac failure; prostate carcinoma	DiI (dissolved)	LFDΓ (2; I–VI; I–VI), RFDΓ (1; I–VI)
10	F	86	24	Pulmonary edema; cardiac failure	DiI (crystalline)	LFCBm (1; I–VI), RFDΓ (1; I–**III**–IV)

Note: M, male; F, female; TDF, time between death and fixation; cytoarchitectonically defined cortical areas FDΓ and FCBm (trans, transition zone between the 2 areas) are based on the description of von Economo and Koskinas (1925) and Amunts et al. (1999) and are preceded by letters L or R for left or right hemisphere, respectively. Roman numerals denote cortical layers, and for large injections the most heavily involved layer is in bold.

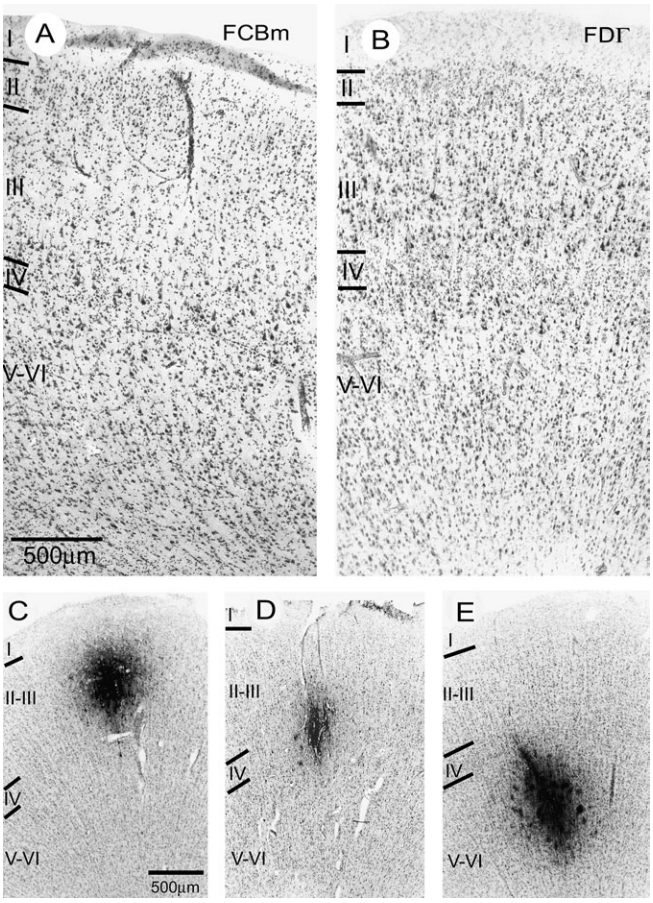

Figure 1. Cytoarchitectonically defined areas FCBm (*A*) and FDΓ (*B*) in Nissl-stained sections. Area FDΓ has a clear layer IV, whereas area FCBm has a dysgranular layer IV invaded by large pyramidal neurons. BDA injections centered in layers II–III (*C*), IV (*D*), and V–VI (*E*).

model VT 1000 S) and collected in a solution of 4% paraformaldehyde in phosphate buffer. Floating sections were stored at 4 °C; for analysis they were mounted on gelatine-coated glass slides in the same fixative, coverslipped, and sealed with nail varnish. After microscopic analysis, the coverslips were removed and the sections were counterstained with cresyl violet.

Analysis

The distribution of axonal and soma labeling was charted using the Lucivid micromonitor (MicroBrightField, Colchester, VT) connected to the microscope and to a PC computer equipped with the Neurolucida software (MicroBrightField). Section contours, limit between the cortex and white matter (visible on noncounterstained sections) and the injection site, were charted using a 10× objective and the distribution of labeled axons and somata outside the injection site with a 40× (BDA sections) or 25× (DiI sections) objectives. After charting, coverslips were removed and sections were counterstained with cresyl violet. Boundaries between cortical layers were added with the same procedure to the charts. For each injection, we determined the maximal spread of connections within the supragranular, granular, and infragranular layers. In order to correct for the relative tangential compression of supragranular layers and the relative expansion of infragranular layers within sulci (and the reverse distortion on gyri), the position of axons most distant from the injection site within each layer was projected into a line running halfway between the upper and lower limits of layer IV, and the maximal spread of connections was measured along this line. The ratio of the extent of infragranular versus supragranular connections (R [V–VI/I–III]) was calculated by dividing the maximal range of intrinsic connections within the infragranular layers by that within the supragranular layers.

Photomicrographs of BDA-labeled elements were taken using a Zeiss microscope (AxioPlan 2) equipped with axiocam digital camera (resolution of 3900 × 3090 pixels) and axiovision software (Zeiss, Feldbach, Switzerland). DiI photomicrographs were taken with confocal laser scanning microscope (Leica TCS NT) using 10×, 25×, 40×, 63×, or 100× objectives. DiI excitation was obtained with an Argon–Krypton laser set at 568 nm, and the emitted light was filtered through an LP 590 filter. For each photomicrograph, stacks of optical sections of 1024 × 1024 pixels spaced 1 µm were collected and projected on a single plane. For photomicrographs, montages were made using the Photoshop 6.0 software (Adobe Systems, San Jose, CA); images were slightly adjusted for brightness and contrast but no other transformations were made.

Results

Eighteen injections were placed in area FDΓ, 10 into area FCBm, and 3 into the transition between them (Table 1), as determined on Nissl-stained sections. Area FCBm is characterized by a dysgranular layer IV invaded by numerous pyramidal neurons, whereas area FDΓ is characterized by a larger and more uniformly granular layer IV (Fig. 1*A*,*B*). Nineteen injections were in layers I–III (Fig. 1*C*), 5 centered in layer IV (Fig. 1*D*), and 3 centered in layers V–VI (Fig. 1*E*). Injections in layer IV were all extending into deep layer III and upper layer V. Four other injections included all cortical layers; 3 of them were made with dissolved DiI and yielded large injection sites of approximately 3 mm diameter and the other one was made with a large DiI crystal. On average, BDA injections (n = 12) yielded smaller injection sites (mean diameter = 470 ± 254 µm) than small DiI crystal placements limited to layers I–III (n = 15; mean diameter = 850 ± 196 µm).

Neuronal and Axonal Types Involved in Intrinsic Connections

DiI tracing led to both antero- and retrograde labeling, whereas BDA (either 3 or 10 kDa; see Table 1) to long-distance anterograde tracing and Golgi-like retrograde labeling in the immediate vicinity of the injection site (Fig. 2*A*,*B*). The analysis of 734 neurons labeled retrogradely following DiI injections in supragranular layers showed that most were located in supragranular layers (90%) and only few in granular (6%) or in infragranular layers (4%), and 98% of them were pyramids.

Both BDA and DiI injections revealed various axonal types. Their diameter varied between 0.3 and 1.5 mm, most were less than 1 µm in diameter and only few thicker. Labeled axons showed various orientations within the cortical layers (Fig. 2*D*–*H*; see also charts in Figs 6 and 7) including horizontally or obliquely oriented axons (Fig. 2*D*,*E*), perpendicularly oriented axons reaching superficial layers (Fig. 2*F*,*G*), or horizontally oriented axons within layer IV (Fig. 2*H*). Regardless of the injected layers, a tight axon bundle ran from the injection site into the white matter (Fig. 2*C*). BDA- and DiI-labeled axons within all cortical layers presented several features such as collaterals (Figs 3*F* and 4*B*) and varicosities resembling terminal (Fig. 3*A*–*C*) or en passant boutons (Fig. 3*D*,*E*). The general patterns of axonal labeling obtained with DiI crystals and BDA were similar.

Tangential Extent of Intrinsic Connections

Large injections of dimethylformamide-dissolved DiI or the placement of a large DiI crystal spread over all cortical layers and labeled numerous axons within the cortex and the

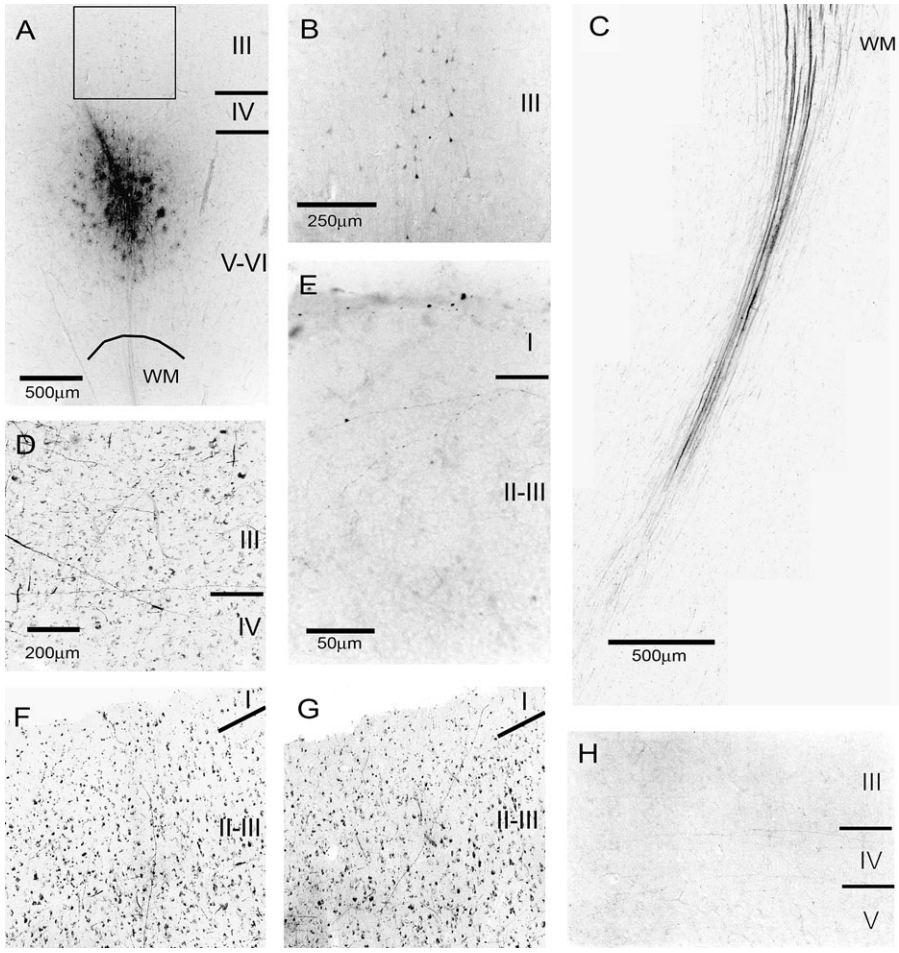

Figure 2. Neuronal and axonal labeling. (*A*) BDA injection in layers V–VI of area FDΓ on the right side yielding retrograde labeling of the above-lying layer III pyramidal neurons (inset in [*A*] is shown at higher magnification in [*B*]). (*C*) Axon bundle within the white matter following DiI injection centered in layer III in area FDΓ on the right side. (*D*) DiI-labeled axons running tangentially and obliquely within layers III and IV following layer III injection in area FDΓ on the left side. (*E*) BDA anterogradely labeled axons in superficial layers following injection in the corresponding layers in area FDΓ on the left side. (*F, G*) Radially oriented axons reaching superficial layers following large DiI injection in area FDΓ on the left side. (*H*) Horizontally running axons within layer IV following layer IV injection with BDA in area FDΓ on the right side. Scale bar in (*F–H*) is the same as in (*D*).

underlying white matter. Outside the injection site, labeled axons were present in all cortical layers with highest density in deep layer III. At distance of approximately 4 mm from the border of the injection site, the density of fibers decreased, and most axons ran parallel to the pial surface. The maximal distance estimated was 8.8 mm from the border of the injection site, obtained with large injections of dissolved DiI. Placement of a large DiI crystal involving all cortical layers yielded axonal labeling at a maximal distance of 6.6 mm. BDA injections lead to similar tracing distances as small DiI crystals when placed in layers I–III (BDA: mean = 2.3 mm, SD = 0.7 mm; DiI: mean = 2.3 mm, SD = 0.8 mm). The maximal spread of connections was within the same range between areas FCBm and FDΓ, and there was no difference between the hemispheres.

Connectivity of Supragranular Layers

Following the placement of crystalline DiI in supragranular layers, neurons and long axons, mostly horizontally oriented, were labeled throughout layer III (Fig. 4*A*). Retrogradely labeled neurons (arrowheads in Fig. 4*A*) were most often medium-size pyramids (ca. 25 µm cell body diameter) with numerous dendritic spines (Fig. 4*D*). In many instances, their main axon was seen to run radially within the cortex (Fig 4*B,C*), giving off horizontal collaterals (arrowheads in Fig. 4*B*) with complex arborizations in deep layer III (Fig. 4*E*). Retrogradely labeled neurons tended to form periodical arrangements (Fig. 4*F*) within layer III. Serial charts of retrogradely labeled neurons revealed clusters of approximately 500 µm diameter located within 3 mm of the injection site, as well as individual neurons as far away as 4 mm from it (Fig. 5).

Placement of crystalline DiI in supragranular layers labeled numerous axons within these layers, the most distant ones at 4.5 mm from the border of the injection site. Serial charts of labeled axons following DiI placement in supragranular layers of area FCBm are shown in Figure 6*A*. In that case, most distant axon segments were located within layers II–III with few fibers in layer IV; in infragranular layers, labeled axons were found mainly below the injection site, including a tight bundle oriented perpendicularly across layers IV–VI and entering the white matter. A similar pattern of axonal labeling was found with a BDA injection in supragranular layers of area FDΓ (Fig. 7*A*). In some other cases, BDA or DiI injections in supragranular layers labeled occasional axons in layer IV and in infragranular layers. The maximal extent of connections found in supragranular, granular, or infragranular layers following 19 injections in supragranular layers of areas FCBm, FDΓ, or the transition

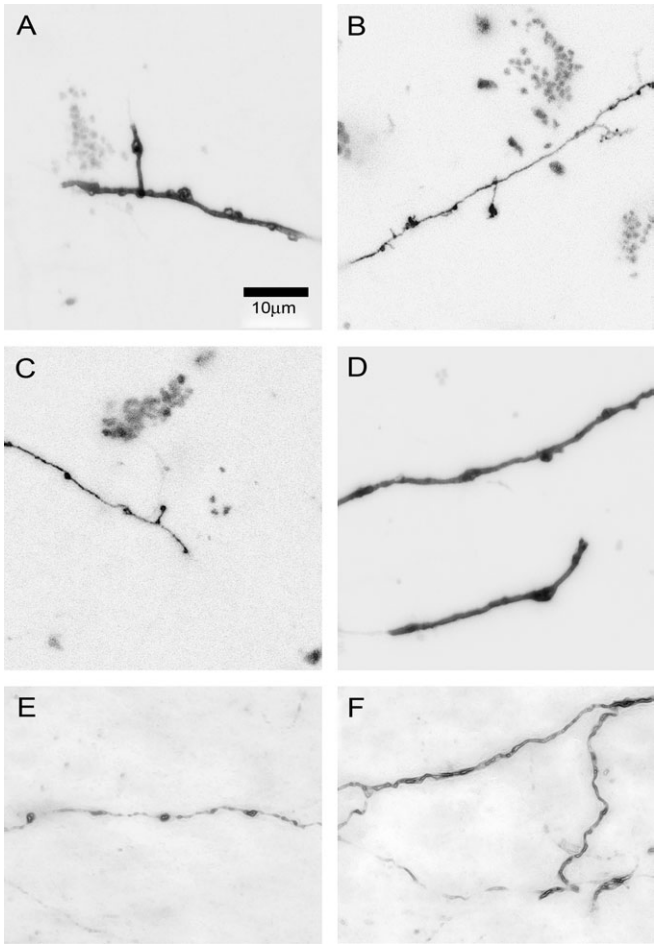

Figure 3. High-magnification photomicrographs showing morphology of labeled axons following DiI (*A–D*) and BDA (*E, F*) injections. (*A–C*) Synaptic-like boutons on short branches resembling terminals. (*D, E*) Axonal varicosities resembling en passant boutons. (*F*) Collateral branchings.

between both is summarized in Table 2. On average, projections tended to be longer within supragranular than the other layers. This was apparent in the ratio between the extent of connections within infragranular versus supragranular layers (R [V–VI/I–III], see Materials and Methods), which was on average below 1.0. Taken individually, 12 of the 19 injections yielded a ratio below 1.0, whereas the other 7 injections had a ratio between 1.0 and 1.2, indicating that in these cases intrinsic connections were extending up to approximately corresponding locations in supra- and infragranular layers. When supragranular injections were grouped according to the hemisphere (left n = 12, right n = 7; as listed in Table 2), left hemisphere injections had a smaller average ratio (0.6 ± 0.4) than right hemisphere injection (0.9 ± 0.3). However, a type-III sum of squares analysis of variance for nonequivalent groups did not reveal significant differences between the 2 hemispheres. The range of intrinsic connections revealed by injections into supragranular layers and its laminar profile were roughly similar in areas FDΓ and FCBm (Table 3).

Connectivity of Layer IV

BDA injections centered on layer IV (n = 5), with a small amount of diffusion in the adjacent deep layer III and upper layer V (e.g., Figs 6*B* and 7*B*), yielded dense axonal labeling within approximately 1.2 mm from the border of the injection site; the average extent of labeling in layer IV varying between 2.2 and 3.1 mm (Table 2). In the vicinity of the injection site, labeled axons were present in deep layer III, in layer IV, and in upper layer V and showed various orientations. A thin compacted axon bundle was running across infragranular layers and entered the white matter. Further away from the injections site, most axons were horizontally oriented and within layer IV (see Fig. 2*H*); the most distant ones were found at 3.7 mm. On average, the projections reached furthest in layer IV (Table 2). The extent of intrinsic connections revealed by injections in layer IV and their laminar profile were roughly similar in FCBm (Fig. 6*B*) and FDΓ (Fig. 7*B*) areas and in the left and right hemisphere.

Connectivity of Infragranular Layers

Following BDA injections centered in infragranular layers (n = 3), labeled axons occupied the injected layers and spread horizontally up to 2.6 mm from the border of the injection site (Figs 6*C* and 7*C*). A thin, compact axon bundle descended radially from the injection site into the white matter. A few axons were also present in granular and supragranular layers, oriented mostly radially, and some reaching upper layer III. The most distant projections from infragranular layers remained within these layers (Table 2), as indicated by the high ratio. As far as we can state from our 3 cases, the extent of intrinsic connections revealed by injections in infragranular layers and their laminar profile were similar in the 2 hemispheres.

Discussion

Intrinsic connections within Broca's area, as demonstrated here for the first time, display 5 characteristic features.

First, they spread tangentially over long distances, as revealed by large injections of dissolved DiI involving all cortical layers. In one of these cases, the maximal tangential spread of intrinsic connections was 8.8 mm, the mean of the 3 cases was 7.4 mm, as compared with maximum range of connections of 1.0–2.3 mm revealed with similar-sized injections in the primary auditory area, 2.5–4.0 mm in auditory areas TB and TA (see Fig. 3 in Tardif and Clarke 2001), or 4 mm in the primary visual area (Burkhalter and Bernardo 1989; Kenan-Vaknin et al. 1992). A comparable range of intrinsic connections (ca. 7 mm) has been reported in the posterior part of Brodmann's area 22, which is, on the left side, part of Wernicke's area (Galuske et al. 2000) and in nonprimary auditory areas for a small number of isolated axons (Tardif and Clarke 2001). The very long projections within Broca's area are rather exceptional because relatively few axon segments were present at 6–8 mm and only after very large injections.

Second, intrinsic connections in Broca's area are formed to 98% by pyramidal neurons. This is similar to what has been found in human auditory and Wernicke's areas (Tardif and Clarke 2001; Galuske et al. 2000) or in nonhuman primate prefrontal cortex (e.g., Kritzer and Goldman-Rakic 1995; Melchitzky et al. 1998). Besides being the origin of intrinsic connections, pyramidal neurons are also likely to be their main recipients, as shown in macaque prefrontal cortex (Melchitzky et al. 1998).

Third, intrinsic connections in Broca's area have a distinct laminar pattern. We have found a strong interconnectivity within the supragranular layers, spreading tangentially over long distances. Supragranular layers were found to send

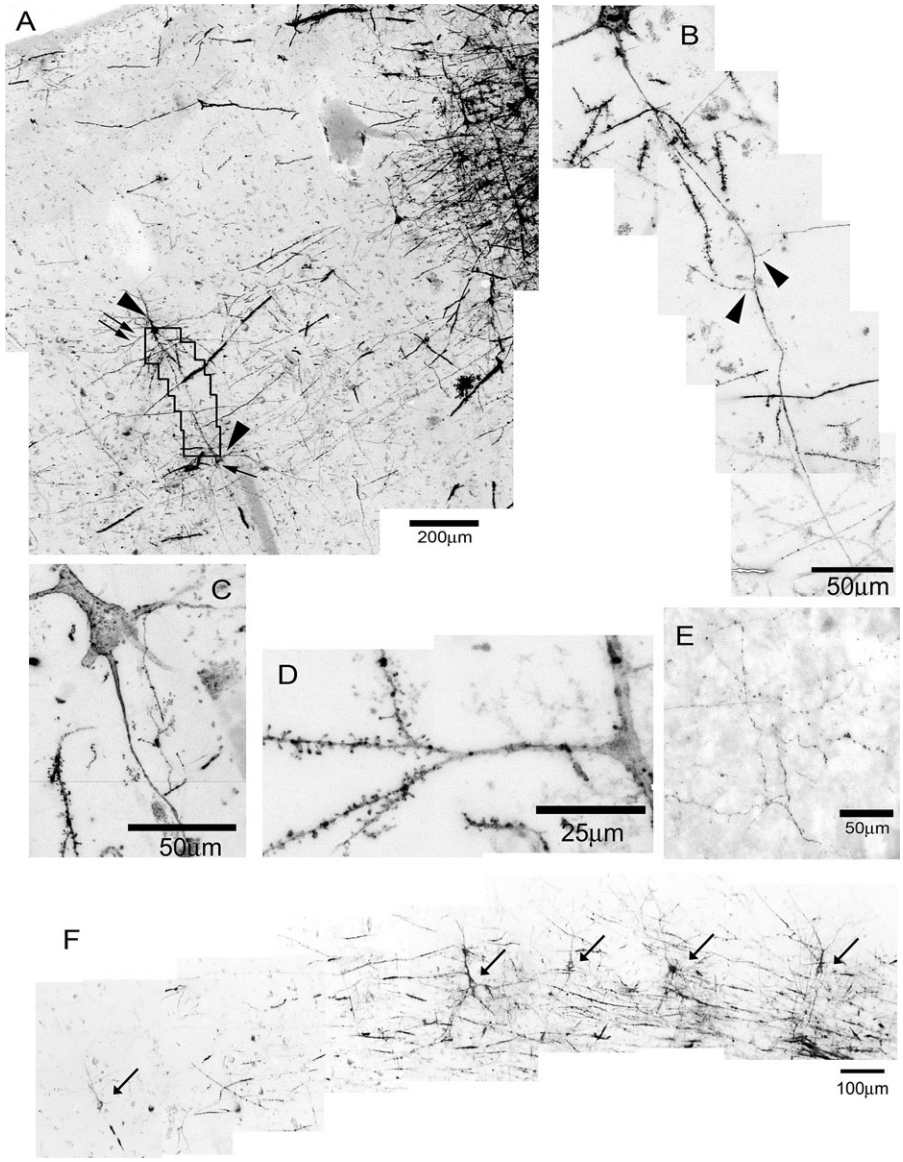

Figure 4. Retrograde and anterograde labeling with DiI (*A–D*, *F*) and BDA (*E*). Small DiI crystal placed in supragranular layers led to both antero- and retrograde labeling. In (*A*), 2 layer III pyramidal neurons (arrowheads) are retrogradely labeled at approximately 1 mm from the border of the injection. (*B*) Higher magnification of the inset in (*A*): descending axon with 2 horizontally oriented collaterals (arrowheads). (*C*) and (*D*) show morphological details of axon initial segment (*C*) and spiny dendrites (*D*), respectively, identified by arrow and double arrow in (*A*). (*E*) Anterograde BDA labeling of axons found in deep layer III. (*F*) Retrogradely labeled pyramidal neurons (arrows) forming periodical arrangement in layer III.

connections to granular and infragranular layers but did not receive massively from them. Furthermore, projections from supra- to infragranular layers tended to remain tangentially more restricted (Fig. 8). Tracing studies in prefrontal areas of nonhuman primates have shown a similar pattern of local connections covering comparable distances: horizontal intrinsic projections within supragranular layers (up to 3–4 mm) exceeded the range of supra- to infragranular projections (about 1 mm; Levitt et al. 1993; Kritzer and Goldman-Rakic 1995; Pucak et al. 1996). Similarly, neurons projecting locally to layer III in area 9 and 46 were mostly located in supragranular layers (up to 7 mm from the injection site) and only few neurons were in infragranular layers (located directly below the injection site; Kritzer and Goldman-Rakic 1995). The small amount of infragranular neurons strikingly contrasts with the large number of infragranular pyramids of the primary visual cortex projecting to layer III (Blasdel et al. 1985; Fitzpatrick et al. 1985; Kisvarday et al. 1989; see also Kritzer and Goldman-Rakic 1995 for a comparison between intrinsic connectivity of prefrontal and primary visual cortices in nonhuman primates). The similarities in intrinsic connectivity in Broca's area and in nonhuman primate prefrontal cortex as well as the difference with that of the primary visual cortex reflect most likely distinct functional specialization of prefrontal versus primary sensory areas in both species.

One surprising result found in the present study concerns the rich axonal network spreading tangentially in layer IV following BDA injections centered on this layer. A similar pattern has been found after injection in layer IV in human and IVC in nonhuman primate primary visual area (Fitzpatrick et al. 1985; Burkhalter

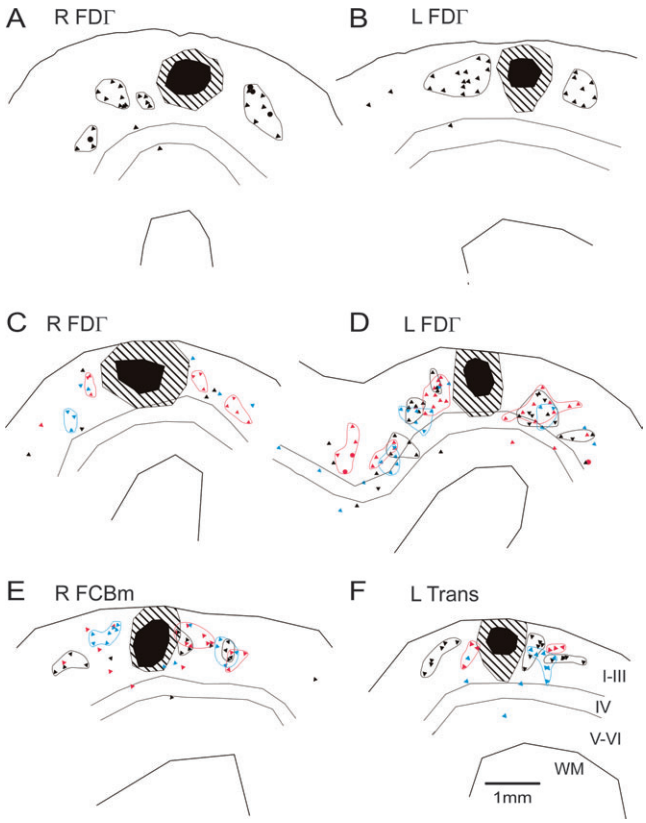

Figure 5. Distribution of retrogradely labeled neurons after DiI injections into layer III of area FDΓ (*A–D*), FCBm (*E*), or transition between them (*F*). In (*A*, *B*), superposed charts of 4 adjacent sections; clusters of neurons are encircled. In (*C–F*), charts of three 300-μm spaced sections are superposed; black lines and symbols refer to the central section, colored symbols to other 2. Clusters of neurons within a given section are encircled by lines of corresponding color. Black area represents the DiI crystal; hatched area, region of diffusion; triangles, pyramidal neurons; circles, unidentified neurons. WM: white matter; L: left hemisphere; R: right hemisphere; Trans: transition zone between areas FDΓ and FCBm.

and Bernardo 1989) but not in the human auditory (Tardif and Clarke 2001), Wernicke's (Galuske et al. 2000), or nonhuman primate prefrontal areas 9 and 46 (Levitt et al. 1993). In the latter study, injections restricted to layer IV lead to a columnar arrangement of projections above and below the injection sites without any apparent horizontal spreading; injections to other layers also failed to label tangentially spreading axons within layer IV (Levitt et al. 1993). Distinct connectivity patterns within layer IV in Broca's area and in areas 9 and 46 of nonhuman primates may reflect species or areal differences.

Fourth, intrinsic connections in Broca's area have a roughly periodic/patchy arrangement, as revealed by the clustered distribution of retrogradely labeled neurons following injections in supragranular layers. In general, the patterns of retrogradely labeled neurons found in the present study were similar to that reported in areas 9 and 46 of rhesus monkeys following layer III injections, both in terms of cluster sizes (500–800 μm) and distances of cell bodies from the injection sites (up to 5–7 mm from the injection site; Kritzer and Goldman-Rakic 1995). However, we did not find patchy distribution of anterogradely labeled axons, either with DiI or BDA injections. In human area 22 of Brodmann, patches formed by retrogradely labeled neurons and anterogradely labeled axons were shown to vary in their mean diameter from 558 to 856 μm (Galuske et al. 2000), which roughly corresponds to sizes of neuron clusters found here and in macaque prefrontal cortex. The clustering of neurons projecting to a specific part of an area suggests a modular organization.

Fifth, intrinsic connections are similar in the 2 cytoarchitectonic subdivisions of Broca's area. In particular, the same laminar pattern of connectivity of supragranular layers was observed in (left) areas FCBm and FDΓ (Table 3). Intrinsic connections in Broca's area tended to differ from those of its counterpart on the right side. Projections originating in supragranular layers tended to spread tangentially wider in supra- than in infragranular layers in Broca's area, whereas they were roughly coextensive in the right hemisphere. However, this difference was not statistically significant, mainly because of a great variability in the extent of right hemispheric projections. Interhemispheric differences were previously shown in Wernicke's area, where the distance between terminal patches in supragranular layers was greater in the left hemisphere (Galuske et al. 2000). We did not observe patchy arrangement of terminals in Broca's area, and the clusters of projecting neurons in supragranular layers (Fig. 5) did not differ between the hemispheres.

Relation to Intrahemispheric Connections

Tracing studies in nonhuman primates have shown that prefrontal areas received afferents from other prefrontal areas (e.g., Barbas and Pandya 1989), from association sensory cortices (e.g., Barbas 1986; Romanski et al. 1999), from areas within the intraparietal sulcus (e.g., Schwartz and Goldman-Rakic 1984), and from the mediodorsal nucleus of the thalamus (e.g., Giguere and Goldman-Rakic 1988; Ray and Price 1993). The laminar distribution of afferents to prefrontal areas has been shown to vary in function of cortical cytoarchitecture. Barbas (Barbas 1986; Barbas and Rempel-Clower 1997) has proposed a classification of cortical areas into 5 levels, strictly referring to the number of identifiable layers and their degree of definition. High-level cortical areas are defined by the presence of clear-cut cortical layers and low-level areas by poor laminar definition with dysgranular layer IV. Projections from high- to low-level areas were shown to originate from layer III and terminate in granular and infragranular layers, whereas projections from low- to high-level areas from infragranular layers and terminate in supragranular layers (Barbas and Rempel-Clower 1997). If a similar organization exists in man, FDΓ, a putative high-level area with well-defined cortical layers, and FCBm, a putative low-level area with dysgranular layer IV, are likely to receive input from different origin in corresponding layers. Thus, intrinsic connections, which were found to be similar in areas FCBm and FDΓ, may be actually involved in the processing of different types of information.

Recently, diffusion-weighted magnetic resonance imaging was used to trace the long-range connections of Broca's area (Anwander et al. 2006; Friederici et al. 2006; Hagmann et al. 2006). Different subregions of Broca's area, potentially corresponding to areas FDΓ, FCBm, and the deep frontal operculum, were found to have different long-range connections (Anwander et al. 2006; Friederici et al. 2006). Furthermore, intra- and interhemispheric connections of Broca's area were shown to display sex- and handedness-related differences (Hagmann et al. 2006). Thus, putative functional differences between the cytoarchitectonic subdivisions of Broca's areas as well as between Broca's area and its right homologue are reflected more in long range rather than intrinsic connectivity.

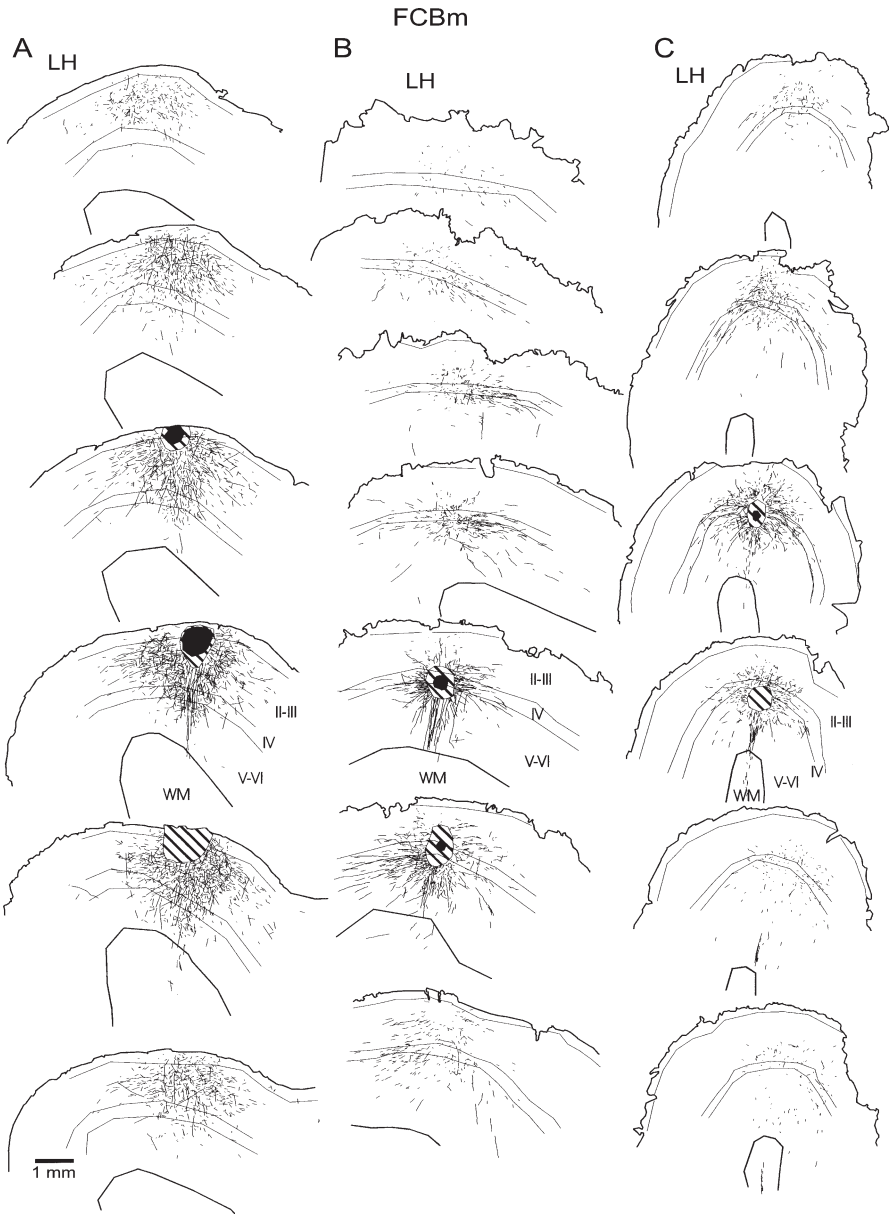

Figure 6. Distribution of labeled axons following DiI (*A*) and BDA (*B, C*) injections in area FCBm. Charted sections are approximately 500-μm spaced. Black area represents the core of the injection and hatched area the region of diffusion. (*A*) DiI injection involving supragranular layers yielded horizontal connections within supragranular layer as well as some projections to infragranular layers below the injection site. (*B*) Injection involving layers IV and superficial V yielded axonal projections within layer IV and in infragranular layers. Some axons segments reached superficial layers above the injection site. (*C*) Injection involving layers IV and V yielded horizontally oriented axons within infragranular layers and layer IV. Labeled axons in supragranular layers were mainly found above the injection site. A thin axon bundle entering the white matter is present for all injections. LH: left hemisphere; WM: white matter.

Technical Considerations

Previous tracing studies in human tissue have been done using several techniques, including horseradish peroxidase (Beach and McGeer 1987, 1988; Haber et al. 1988), biocytin (Kenan-Vaknin et al. 1992), neurobiotin and BDA (Dai, Swaab, et al. 1998; Dai et al. 1998a, 1998b; Tardif et al. 2005), DiI (Burkhalter and Bernardo 1989; Mufson et al. 1990; Burkhalter 1993; Burkhalter et al. 1993; Lim et al. 1997; Galuske et al. 2000; Tardif and Clarke 2001, 2002; Tardif et al. 2005), or the Nauta method (Mesulam 1979; Clarke and Miklossy 1990; Clarke 1994; Di Virgilio and Clarke 1997; Clarke et al. 1999; Di Virgilio et al. 1999; Wiesendanger et al. 2004). Results obtained in the present study suggest that BDA and DiI can bring complementary information on intrinsic cortical connectivity. Large DiI injections into fixed material can trace relatively long connections (up to 8.8 mm in the present study) and, for intrinsic cortical connections, the pattern of connections originating from all cortical layers. Placement of DiI crystals yields much smaller injection sites and reveals the projection pattern arising from specific layers, here supragranular layers. DiI reveals well morphological features of axons, such as terminal-like or en passant boutons and of neurons that are retrogradely labeled in a Gogi-like fashion. Iontophoretic BDA injections into fresh, nonfixed tissue allow more confined injections, which can target particular cortical layers. Moreover, it allows tracing distance up to approximately 4 mm within 12 h, whereas DiI

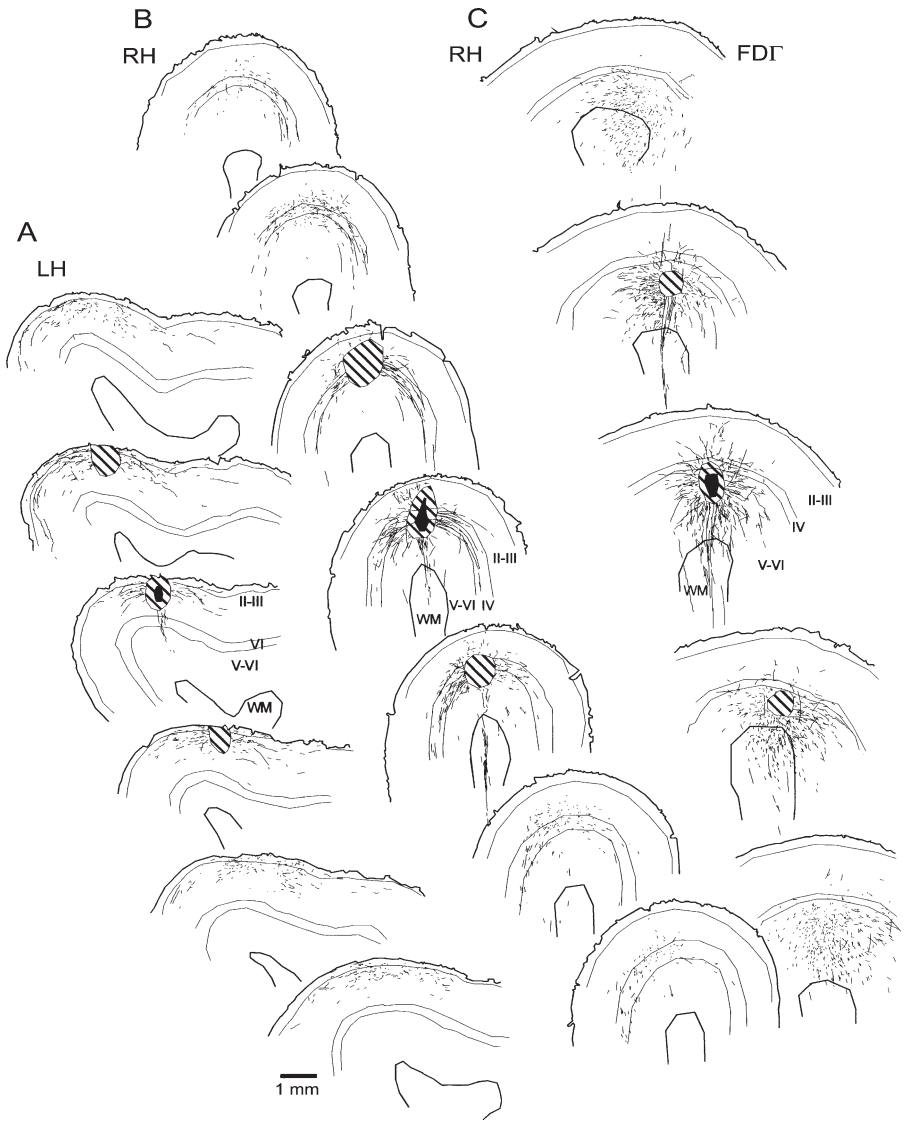

Figure 7. Distribution of labeled axons following BDA injections in area FDΓ. (*A*) Injection in supragranular layers yielded long-range horizontal fibers located in the same layers. (*B*) Injection centered in layer IV but extending also to layers III and V yielded long horizontal projections within layer IV. (*C*) Injection in infragranular layers (encroaching also on layer IV) yielded projections mostly within the infragranular layers with a few vertically oriented axons reaching supragranular layers above the injection site. LH: left hemisphere; RH: right hemisphere. Same conventions as in Figure 6.

tracing of similar distance requires several weeks (Lukas et al. 1998). In vivo studies in animals reported that BDA 3 and 10 kDa were transported retro- and anterogradely, respectively (Reiner et al. 2000), which was not the case in postmortem human material.

General Conclusions

The present study shows that long horizontal intrinsic connections exist within Broca's area and are mainly formed by axons of pyramidal neurons located within supragranular layers. Neurons forming intra- and interlaminar connections tend to be grouped into clusters suggesting modular organization. By opposition to what was previously shown in primary visual cortex, only few neurons project from infra- to supragranular layers in Broca's area. An extensive tangential network of projections exists within layer IV in contrast with the intrinsic organization of prefrontal areas of nonhuman primates. The

Table 2
Extent of intrinsic connections

Injections in layers	I–VI		I–III		IV		V–VI	
	Left	Right	Left	Right	Left	Right	Left	Right
Maximal range in layers								
I–III	7.4 ± 1.2	5.9	2.1 ± 0.5	2.2 ± 1.1	2.0 ± 0.2	1.8 ± 0.2	1.7 ± 0.6	1.1
IV	7.4 ± 1.2	5.9	1.3 ± 0.9	1.9 ± 1.3	2.2 ± 0.9	3.1 ± 0.9	1.9 ± 0.6	1.1
V–VI	7.4 ± 1.2	5.9	1.1 ± 0.8	2.0 ± 1.2	1.3 ± 0.6	2.2 ± 0.1	2.6 ± 0.1	2.3
R (V–VI/I–III)	1.0±0.0	1.0	0.6±0.4	0.9±0.3	0.6±0.2	1.2±0.2	1.7 ± 0.7	2.1
n	3	1	12	7	3	2	2	1

Note: Maximal extent of intrinsic connections (mean ± SD; in millimeter) within layers I–III, IV, and V–VI following injections into areas FCBm, FDΓ, or the transition zone between both, involving all cortical layers (I–VI) or limited to layers I–III, IV, or V–VI. The extent of supra- versus infragranular connections (ratio, R) was obtained for each individual injection by dividing the maximal mean range of intrinsic connections within infragranular layers by that within supragranular layers; the mean (±SD) is listed here.

Table 3
Extent of intrinsic connections in cytoarchitectonic areas

Injections in layers I–III

	FCBm		FDΓ	
	Left	Right	Left	Right
Maximal range in layers				
I–III	2.3 ± 0.2	1.7 ± 0.4	2.0 ± 0.6	3.0 ± 1.5
IV	1.1 ± 0.4	1.6 ± 0.7	1.4 ± 0.9	2.4 ± 1.9
V–VI	0.8 ± 0.3	1.6 ± 0.7	1.3 ± 0.8	2.5 ± 1.7
R (V–VI/I–III)	0.4 ± 0.1	0.9 ± 0.3	0.7 ± 0.4	0.8 ± 0.3
n	2	4	8	3

Note: Maximal extent of intrinsic connections (mean ± SD; in millimeter) within layers I–III, IV, and V–VI following injections limited to layers I–III. Data come from the same injections as in Table 2 but are listed according to the cytoarchitectonic areas injected and limited to supragranular injections. These data are from a subset of injections presented in Table 2; 2 injections into the transition zone between the 2 areas are not listed here. Same conventions as in Table 2.

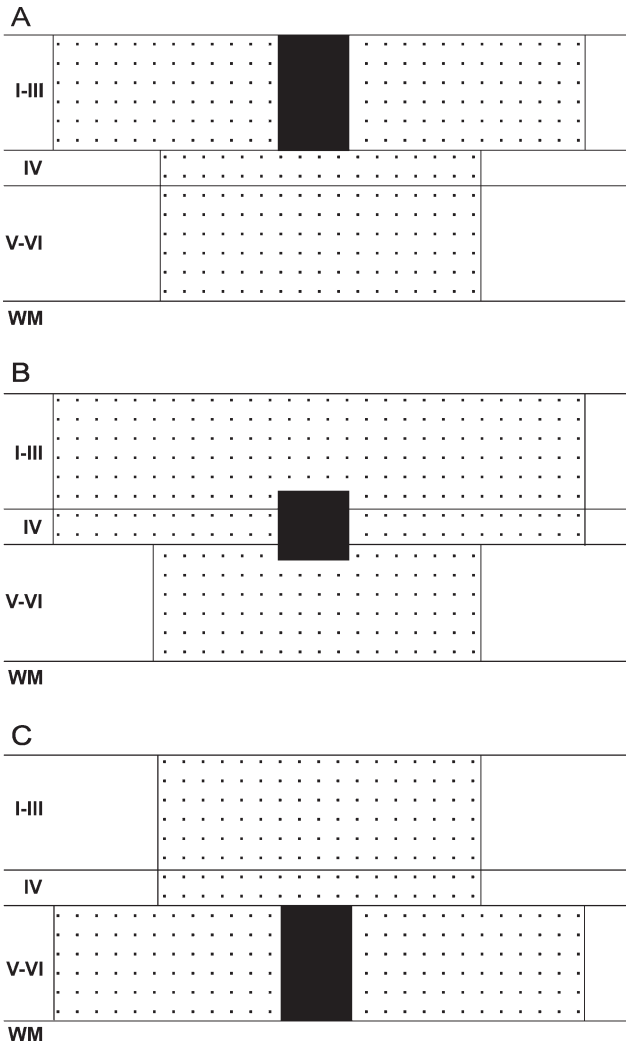

Figure 8. Schematic representation of laminar contributions to intrinsic connections within Broca's area. A distinct location within the supragranular layers (indicated by the black rectangle in [*A*]) is interconnected widely within the same layers and more narrowly with granular and infragranular layers. A distinct location in the granular layer (*B*) is interconnected widely within supragranular and granular layers and narrowly with infragranular layers. A distinct location in infragranular layers (*C*) is interconnected widely within the same layers and narrowly with supragranular and granular layers.

overall pattern of intrinsic connectivity is similar between the 2 hemispheres as well as between the 2 cytoarchitectonic constituent areas.

Notes

We are very grateful to Mrs B. Delacuisine for excellent histological assistance, to Mr R. Kraftsik and Mr E. Bernardi for advice and help with photography and image processing, and to Mr C. Haeberli for constructing the iontophoretic apparatus. This work has been supported by the Swiss National Science Foundation grants 3100-103895 and RATP (Réseaux à axes thématiques prioritaires) to S.C. *Conflict of Interest*: None declared.

Address correspondence to Prof S. Clarke, Service de Neuropsychologie et de Neuroréhabilitation, CHUV, Université de Lausanne, 1011 Lausanne, Switzerland. Email: stephanie.clarke@chuv.ch.

References

Amunts K, Schleicher A, Burgel U, Mohlberg H, Uylings HB, Zilles K. 1999. Broca's region revisited: cytoarchitecture and intersubject variability. J Comp Neurol. 412:319–341.

Amunts K, Schleicher A, Ditterich A, Zilles K. 2003. Broca's region: cytoarchitectonic asymmetry and developmental changes. J Comp Neurol. 465:72–89.

Anwander A, Tittgemeyer M, von Cramon DY, Friederici AD, Knosche TR. 2006. Connectivity-based parcellation of Broca's area. Cereb Cortex. 17:816–825.

Aziz-Zadeh L, Koski L, Zaidel E, Mazziotta J, Iacoboni M. 2006. Lateralization of the human mirror neuron system. J Neurosci. 26:2964–2970.

Barbas H. 1986. Pattern in the laminar origin of corticocortical connections. J Comp Neurol. 252:415–422.

Barbas H, Pandya DN. 1989. Architecture and intrinsic connections of the prefrontal cortex in the rhesus monkey. J Comp Neurol. 286:353–375.

Barbas H, Rempel-Clower N. 1997. Cortical structure predicts the pattern of corticocortical connections. Cereb Cortex. 7:635–646.

Beach TG, McGeer EG. 1987. Tract-tracing with horseradish peroxidase in the postmortem human brain. Neurosci Lett. 76:37–41.

Beach TG, McGeer EG. 1988. Retrograde filling of pyramidal neurons in postmortem human cerebral cortex using horseradish peroxidase. J Neurosci Methods. 23:187–193.

Binkofski F, Amunts K, Stephan KM, Posse S, Schormann T, Freund HJ, Zilles K, Seitz RJ. 2000. Broca's region subserves imagery of motion: a combined cytoarchitectonic and fMRI study. Hum Brain Mapp. 11:273–285.

Binkofski F, Buccino G. 2004. Motor functions of the Broca's region. Brain Lang. 89:362–369.

Blasdel GG, Lund JS, Fitzpatrick D. 1985. Intrinsic connections of macaque striate cortex: axonal projections of cells outside lamina 4C. J Neurosci. 5:3350–3369.

Bookheimer S. 2002. Functional MRI of language: new approaches to understanding the cortical organization of semantic processing. Annu Rev Neurosci. 25:151–188.

Bottini G, Corcoran R, Sterzi R, Paulesu E, Schenone P, Scarpa P, Frackowiak RS, Frith CD. 1994. The role of the right hemisphere in the interpretation of figurative aspects of language. A positron emission tomography activation study. Brain. 117(Pt 6):1241–1253.

Braak H. 1979. The pigment architecture of the human frontal lobe. I. Precentral, subcentral and frontal region. Anat Embryol (Berlin). 157:35–68.

Broca P. 1861. Nouvelle observation d'aphémie produite par une lésion de la moitie postérieure des deuxième et troisième circonvolutions frontales. Bull Soc Anat Paris. 6:398–407.

Brodmann K. 1909. Vergleichende Localisationslehre der Grosshirnrinde in ihren Prinzipien dargestellt auf Grund des Zellenbaues. Leipzig (Germany): Johann Ambrosius Barth.

Buchanan TW, Lutz K, Mirzazade S, Specht K, Shah NJ, Zilles K, Jancke L. 2000. Recognition of emotional prosody and verbal components of

spoken language: an fMRI study. Brain Res Cogn Brain Res. 9:227–238.
Burkhalter A. 1993. Development of forward and feedback connections between areas V1 and V2 of human visual cortex. Cereb Cortex. 3:476–487.
Burkhalter A, Bernardo KL. 1989. Organization of corticocortical connections in human visual cortex. Proc Natl Acad Sci USA. 86:1071–1075.
Burkhalter A, Bernardo KL, Charles V. 1993. Development of local circuits in human visual cortex. J Neurosci. 13:1916–1931.
Caplan R, Dapretto M. 2001. Making sense during conversation: an fMRI study. Neuroreport. 12:3625–3632.
Carr L, Iacoboni M, Dubeau MC, Mazziotta JC, Lenzi GL. 2003. Neural mechanisms of empathy in humans: a relay from neural systems for imitation to limbic areas. Proc Natl Acad Sci USA. 100:5497–5502.
Chaminade T, Meary D, Orliaguet JP, Decety J. 2001. Is perceptual anticipation a motor simulation? A PET study. Neuroreport. 12:3669–3674.
Clarke S. 1994. Association and intrinsic connections of human extrastriate visual cortex. Proc Biol Sci. 257:87–92.
Clarke S, Miklossy J. 1990. Occipital cortex in man: organization of callosal connections, related myelo- and cytoarchitecture, and putative boundaries of functional visual areas. J Comp Neurol. 298:188–214.
Clarke S, Riahi-Arya S, Tardif E, Eskenasy AC, Probst A. 1999. Thalamic projections of the fusiform gyrus in man. Eur J Neurosci. 11:1835–1838.
Dai J, Swaab DF, Van der Vliet J, Buijs RM. 1998. Postmortem tracing reveals the organization of hypothalamic projections of the suprachiasmatic nucleus in the human brain. J Comp Neurol. 400:87–102.
Dai J, Van der Vliet J, Swaab DF, Buijs RM. 1998a. Human retinohypothalamic tract as revealed by in vitro postmortem tracing. J Comp Neurol. 397:357–370.
Dai J, Van Der Vliet J, Swaab DF, Buijs RM. 1998b. Postmortem anterograde tracing of intrahypothalamic projections of the human dorsomedial nucleus of the hypothalamus. J Comp Neurol. 401:16–33.
Di Virgilio G, Clarke S. 1997. Direct interhemispheric visual input to human speech areas. Hum Brain Mapp. 5:347–354.
Di Virgilio G, Clarke S, Pizzolato G, Schaffner T. 1999. Cortical regions contributing to the anterior commissure in man. Exp Brain Res. 124:1–7.
Fitzpatrick D, Lund JS, Blasdel GG. 1985. Intrinsic connections of macaque striate cortex: afferent and efferent connections of lamina 4C. J Neurosci. 5:3329–3349.
Foundas AL. 1995. Language dominance and MRI asymmetries. Neurology. 45:1635–1636.
Foundas AL, Eure KF, Luevano LF, Weinberger DR. 1998. MRI asymmetries of Broca's area: the pars triangularis and pars opercularis. Brain Lang. 64:282–296.
Foundas AL, Leonard CM, Gilmore RL, Fennell EB, Heilman KM. 1996. Pars triangularis asymmetry and language dominance. Proc Natl Acad Sci USA. 93:719–722.
Foundas AL, Weisberg A, Browning CA, Weinberger DR. 2001. Morphology of the frontal operculum: a volumetric magnetic resonance imaging study of the pars triangularis. J Neuroimaging. 11:153–159.
Friederici AD. 2001. Syntactic, prosodic, and semantic processes in the brain: evidence from event-related neuroimaging. J Psycholinguist Res. 30:237–250.
Friederici AD, Bahlmann J, Heim S, Schubotz RI, Anwander A. 2006. The brain differentiates human and non-human grammars: functional localization and structural connectivity. Proc Natl Acad Sci USA. 103:2458–2463.
Galaburda AM. 1980. Broca's region: anatomic remarks made a century after the death of its discoverer. Rev Neurol (Paris). 136:609–616.
Galuske RA, Schlote W, Bratzke H, Singer W. 2000. Interhemispheric asymmetries of the modular structure in human temporal cortex. Science. 289:1946–1949.
Giguere M, Goldman-Rakic PS. 1988. Mediodorsal nucleus: areal, laminar, and tangential distribution of afferents and efferents in the frontal lobe of rhesus monkeys. J Comp Neurol. 277:195–213.
Grafton ST, Hazeltine E, Ivry RB. 2002. Motor sequence learning with the nondominant left hand. A PET functional imaging study. Exp Brain Res. 146:369–378.
Haber S. 1988. Tracing intrinsic fiber connections in postmortem human brain with WGA-HRP. J Neurosci Methods. 23:15–22.
Hagmann P, Cammoun L, Martuzzi R, Maeder P, Clarke S, Thiran JP, Meuli R. 2006. Hand preference and sex shape the architecture of language networks. Hum Brain Mapp. 27:828–835.
Hagoort P. 2005. On Broca, brain, and binding: a new framework. Trends Cogn Sci. 9:416–423.
Hayes TL, Lewis DA. 1995. Anatomical specialization of the anterior motor speech area: hemispheric differences in magnopyramidal neurons. Brain Lang. 49:289–308.
Heiser M, Iacoboni M, Maeda F, Marcus J, Mazziotta JC. 2003. The essential role of Broca's area in imitation. Eur J Neurosci. 17:1123–1128.
Horwitz B, Amunts K, Bhattacharyya R, Patkin D, Jeffries K, Zilles K, Braun AR. 2003. Activation of Broca's area during the production of spoken and signed language: a combined cytoarchitectonic mapping and PET analysis. Neuropsychologia. 41:1868–1876.
Hutsler J, Galuske RA. 2003. Hemispheric asymmetries in cerebral cortical networks. Trends Neurosci. 26:429–435.
Iacoboni M, Woods RP, Brass M, Bekkering H, Mazziotta JC, Rizzolatti G. 1999. Cortical mechanisms of human imitation. Science. 286:2526–2528.
Kang AM, Constable RT, Gore JC, Avrutin S. 1999. An event-related fMRI study of implicit phrase-level syntactic and semantic processing. Neuroimage. 10:555–561.
Kenan-Vaknin G, Ouaknine GE, Razon N, Malach R. 1992. Organization of layers II-III connections in human visual cortex revealed by in vitro injections of biocytin. Brain Res. 594:339–342.
Kisvarday ZF, Cowey A, Smith AD, Somogyi P. 1989. Interlaminar and lateral excitatory amino acid connections in the striate cortex of monkey. J Neurosci. 9:667–682.
Koski L, Iacoboni M, Dubeau MC, Woods RP, Mazziotta JC. 2003. Modulation of cortical activity during different imitative behaviors. J Neurophysiol. 89:460–471.
Koski L, Wohlschlager A, Bekkering H, Woods RP, Dubeau MC, Mazziotta JC, Iacoboni M. 2002. Modulation of motor and premotor activity during imitation of target-directed actions. Cereb Cortex. 12:847–855.
Kritzer MF, Goldman-Rakic PS. 1995. Intrinsic circuit organization of the major layers and sublayers of the dorsolateral prefrontal cortex in the rhesus monkey. J Comp Neurol. 359:131–143.
Leslie KR, Johnson-Frey SH, Grafton ST. 2004. Functional imaging of face and hand imitation: towards a motor theory of empathy. Neuroimage. 21:601–607.
Levitt JB, Lewis DA, Yoshioka T, Lund JS. 1993. Topography of pyramidal neuron intrinsic connections in macaque monkey prefrontal cortex (areas 9 and 46). J Comp Neurol. 338:360–376.
Lim C, Mufson EJ, Kordower JH, Blume HW, Madsen JR, Saper CB. 1997. Connections of the hippocampal formation in humans: II. The endfolial fiber pathway. J Comp Neurol. 385:352–371.
Livingstone MS, Hubel DH. 1984. Specificity of intrinsic connections in primate primary visual cortex. J Neurosci. 4:2830–2835.
Lukas JR, Aigner M, Denk M, Heinzl H, Burian M, Mayr R. 1998. Carbocyanine postmortem neuronal tracing. Influence of different parameters on tracing distance and combination with immunocytochemistry. J Histochem Cytochem. 46:901–910.
Lund JS, Yoshioka T, Levitt JB. 1993. Comparison of intrinsic connectivity in different areas of macaque monkey cerebral cortex. Cereb Cortex. 3:148–162.
Maess B, Koelsch S, Gunter TC, Friederici AD. 2001. Musical syntax is processed in Broca's area: an MEG study. Nat Neurosci. 4:540–545.
Mecklinger A, Gruenewald C, Besson M, Magnie MN, Von Cramon DY. 2002. Separable neuronal circuitries for manipulable and non-manipulable objects in working memory. Cereb Cortex. 12:1115–1123.
Melchitzky DS, Sesack SR, Pucak ML, Lewis DA. 1998. Synaptic targets of pyramidal neurons providing intrinsic horizontal connections in monkey prefrontal cortex. J Comp Neurol. 390:211–224.

Mesulam MM. 1979. Tracing neural connections of human brain with selective silver impregnation. Observations on geniculocalcarine, spinothalamic, and entorhinal pathways. Arch Neurol. 36:814–818.
Mufson EJ, Brady DR, Kordower JH. 1990. Tracing neuronal connections in postmortem human hippocampal complex with the carbocyanine dye DiI. Neurobiol Aging. 11:649–653.
Muller RA, Kleinhans N, Courchesne E. 2001. Broca's area and the discrimination of frequency transitions: a functional MRI study. Brain Lang. 76:70–76.
Price CJ. 2000. The anatomy of language: contributions from functional neuroimaging. J Anat. 197(Pt 3):335–359.
Pucak ML, Levitt JB, Lund JS, Lewis DA. 1996. Patterns of intrinsic and associational circuitry in monkey prefrontal cortex. J Comp Neurol. 376:614–630.
Rao SM, Harrington DL, Haaland KY, Bobholz JA, Cox RW, Binder JR. 1997. Distributed neural systems underlying the timing of movements. J Neurosci. 17:5528–5535.
Ray JP, Price JL. 1993. The organization of projections from the mediodorsal nucleus of the thalamus to orbital and medial prefrontal cortex in macaque monkeys. J Comp Neurol. 337:1–31.
Reiner A, Veenman CL, Medina L, Jiao Y, Del Mar N, Honig MG. 2000. Pathway tracing using biotinylated dextran amines. J Neurosci Methods. 103:23–37.
Rizzolatti G, Arbib MA. 1998. Language within our grasp. Trends Neurosci. 21:188–194.
Rockland KS, Lund JS. 1983. Intrinsic laminar lattice connections in primate visual cortex. J Comp Neurol. 216:303–318.
Romanski LM, Tian B, Fritz J, Mishkin M, Goldman-Rakic PS, Rauschecker JP. 1999. Dual streams of auditory afferents target multiple domains in the primate prefrontal cortex. Nat Neurosci. 2:1131–1136.
Schubotz RI, Friederici AD, von Cramon DY. 2000. Time perception and motor timing: a common cortical and subcortical basis revealed by fMRI. Neuroimage. 11:1–12.
Schubotz RI, von Cramon DY. 2001. Functional organization of the lateral premotor cortex: fMRI reveals different regions activated by anticipation of object properties, location and speed. Brain Res Cogn Brain Res. 11:97–112.
Schwartz ML, Goldman-Rakic PS. 1984. Callosal and intrahemispheric connectivity of the prefrontal association cortex in rhesus monkey: relation between intraparietal and principal sulcal cortex. J Comp Neurol. 226:403–420.
Tardif E, Clarke S. 2001. Intrinsic connectivity of human auditory areas: a tracing study with DiI. Eur J Neurosci. 13:1045–1050.
Tardif E, Clarke S. 2002. Commissural connections of human superior colliculus. Neuroscience. 111:363–372.
Tardif E, Delacuisine B, Probst A, Clarke S. 2005. Intrinsic connectivity of human superior colliculus. Exp Brain Res. 166:316–324.
Vigneau M, Beaucousin V, Herve PY, Duffau H, Crivello F, Houde O, Mazoyer B, Tzourio-Mazoyer N. 2006. Meta-analyzing left hemisphere language areas: phonology, semantics, and sentence processing. Neuroimage. 30:1414–1432.
von Economo C, Koskinas GN. 1925. Die Cytoarchitektonik der Hirnrinde des erwachsenen Menschen. Vienna/Berlin (Germany): Springer.
Wiesendanger E, Clarke S, Kraftsik R, Tardif E. 2004. Topography of cortico-striatal connections in man: anatomical evidence for parallel organization. Eur J Neurosci. 20:1915–1922.